Université de Mons
**Faculté Polytechnique – Service de Mécanique Rationnelle, Dynamique et Vibrations**
31, Bld Dolez - B-7000 MONS (Belgique)
065/37 42 15 – georges.kouroussis@umons.ac.be


G. Kouroussis, D. Ainalis, S. Zhu, W. Zhai, Mitigation measures for urban railway-induced ground vibrations using dynamic vibration absorbers, *Proceedings of the 25th International Congress on Sound and Vibration*, Hiroshima (Japan), July 8–12, 2018.

25th International Congress on Sound and Vibration
8-12 July 2018 HIROSHIMA CALLING
ICSV25

# MITIGATION MEASURES FOR URBAN RAILWAY-INDUCED GROUND VIBRATIONS USING DYNAMIC VIBRATION ABSORBERS

Georges Kouroussis, Daniel Ainalis
*University of Mons, Faculty of Engineering, Department of Theoretical Mechanics, Dynamics and Vibrations, Mons, Belgium*
*email: georges.kouroussis@umons.ac.be*

Shengyang Zhu, Wanming Zhai
*Southwest Jiaotong University, Train and Track Research Institute, State Key Laboratory of Traction Power, Chengdu, People's Republic of China*

Railway-induced ground vibration remains an important showstopper, especially in urban areas where significant levels of vibration are felt by residents. This paper presents a theoretical study of mitigation measures based on the use of Dynamic Vibration Absorbers (DVAs). Such devices can be tuned to a specific excitation frequency in order to reduce the forced response by absorbing the corresponding vibration resonance. The presented work focuses on the specific case of the T2000 tram circulating in Brussels, where large magnitudes of vibration are recorded during the passing over localized rail joints and turnouts. In order to design the DVAs, a numerical model is established, based on a recently developed two-step approach, which includes a coupled multibody model for the vehicle and a finite element/lumped mass model for the track. The model is completed with a 3D finite element model of the soil to simulate the ground wave propagation generated from the dynamic interaction between the vehicle and the track and can be used to evaluate the vibration level in the surrounding area. Tuned DVAs are also modelled, taking into account the design of each element. Finally, several comparisons are performed to quantify their efficiency and determine whether they are more effective in the vehicle or on the track.

Keywords: dynamic vibration absorber, turnout, rail joint, ground vibration, Brussels tram

## 1. Introduction

The generation of railway ground-borne vibrations is a consequence of the vehicle forces passing from the rotating wheels into the track. These forces depend on the moving vehicle's weight (static contribution, often called quasi-static effect) and on the surface irregularities at the wheel and rail surfaces (representing the dynamic contribution of the whole system). They both contribute to the propagation of vibrations outwards from the track [1]. The vibration level experienced is a function of this force, depending on the amplification factors of each track and soil component (and all other locations within the track, soil or nearby structures), and the excitation frequency. Therefore, it is imperative that both effects are well evaluated in the ground vibration assessment [2]. The vibration generated by the railway depends on the type of vehicle (or network) and the quality of the rolling surface. To understand the generation and the propagation of vibrations generated by trains when passing on localized defects (e.g. turnout, as illustrated in Fig. 1 where different singular defects can be observed along the rail direction), it is reasonable to consider that the main contributor to railway vibration is the single force acting on the wheel/rail-defect contact point.

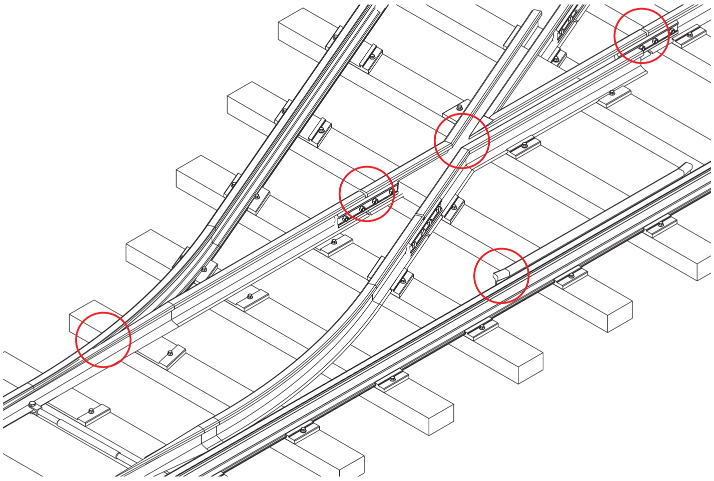

Figure 1: Turnout along which possible localized surface defects on rail are present (circled).

Many mitigation approaches have been studied in recent years, including measures close to the source of excitation (e.g. floating slab, rail suspension fasteners or within the vehicle) or along the propagation path (e.g. wave impeding blocks, trenches or wave barrier). The case of light rail transit networks in urban conditions is likely to be found many examples [3]. The most challenging part to evaluate such antivibration solutions is their validation prior to execution. In this way, environmental vibration prediction models offer a means to quantify their effectiveness. By focusing on actions on the vehicle or the track, numerical modelling is suitable for performing parametric studies. For example, comprehensive vehicle/track/soil models (e.g. [4]) or hybrid numerical/experimental approaches (e.g. [5]) have shown their efficiency to quantify the vibrations generated by localized defects. Both approaches are complementary, depending on whether or not the soil information is parametrized.

This paper aims to investigate the possibility of using Dynamic Vibration Absorbers (DVAs) to mitigate the vibration in urban areas, due to the presence of a localized defect. To do this, a case study using the T2000 tram is undertaken. After analysing the possible frequency range responsible for large ground vibration amplitude, the mathematical development of DVA tuning is presented. A validated numerical model is finally used to assess the best location of the DVA, either on the vehicle (carbodies, bogies, wheels) or on the track.

## 2. Case study: the T2000 tram

The T2000 tram is a medium-sized system running in Brussels. The6 tram progressively replaced the old PCC7000 trams circulating in Brussels Region since the nineties. Figure 2 presents the vehicle configuration, composed of a small centre car surrounded by two large cars. Some technical particularities can be highlighted: the central car body is supported by a classical rigid bogie (BR4$\times$4bogie), composed of four independent drive wheels. The leading cars have an articulated frame at the extremities allowing each wheel to be tangential to the rail (BA2000 bogie). It is made up of two independent rotating wheels driven by a motor inside the wheels, along two trailer wheels. Each drive wheel is powered by a geared motor mounted inside the wheels. Each with geared motor is equipped with resilient wheels that are characterized by a rubber layer inserted between the web and the tread, composed of viscoelastic pads arranged in pairs circumferentially.

The low-floor and large unsprung mass design typically generates large ground vibrations, especially at low speeds and when passing on localized defects [4, 6]. Figure 3 shows the numerical results obtained from a full comprehensive vehicle/track/soil model [7] for the excitation force at the

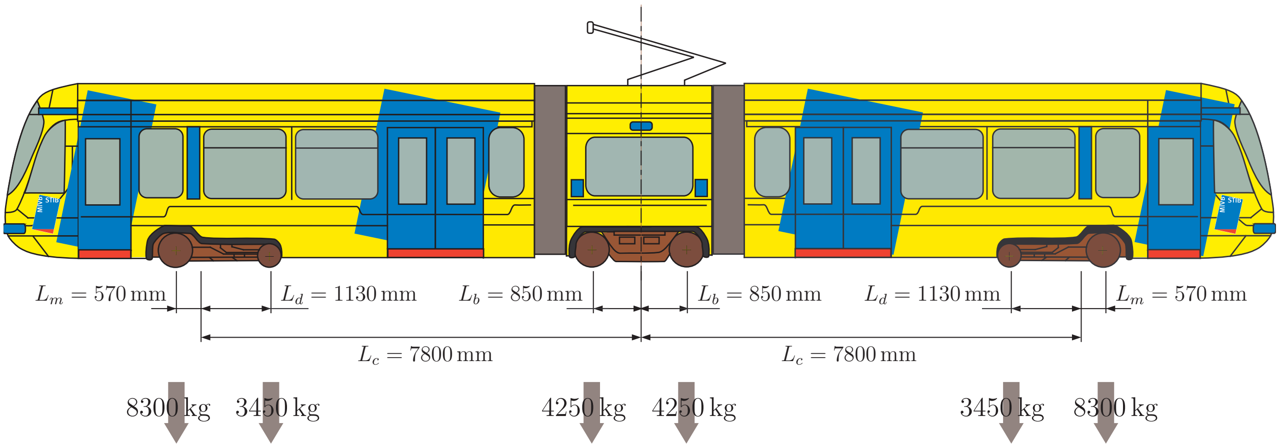


Figure 2: Main dimensions and axle loads of the T2000 tram.

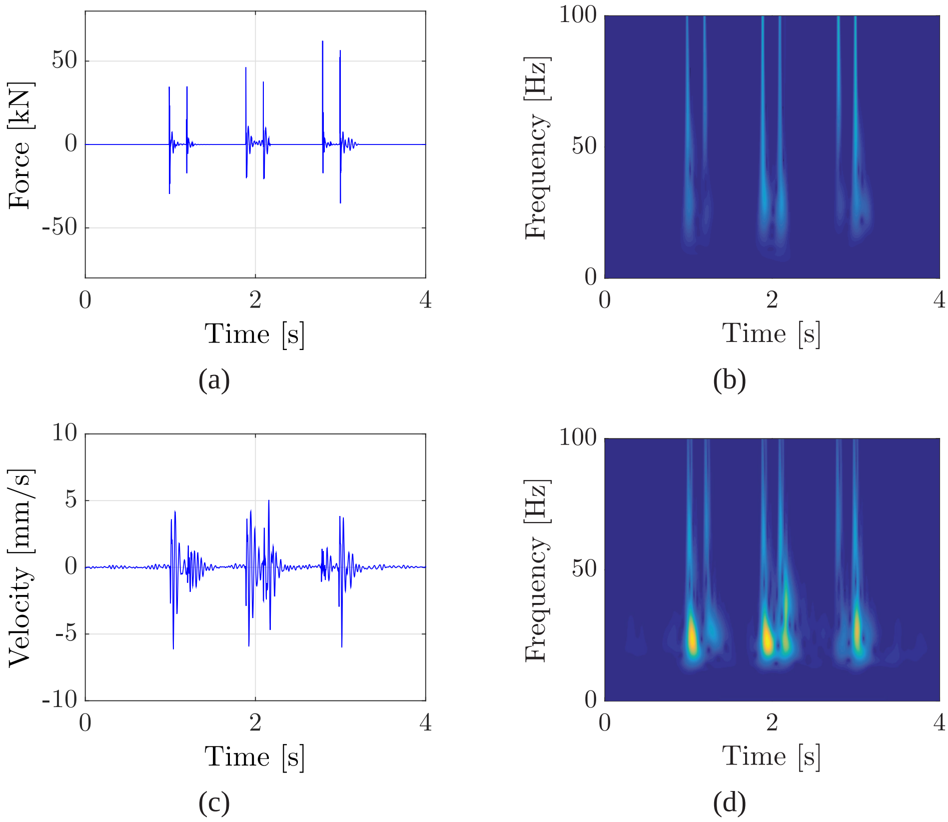


Figure 3: Numerical results of the T2000 tram passing over a singular defect at a speed of $30\,\mathrm{km/h}$ : (a) time history of wheel/rail contact force, (b) corresponding time-frequency force amplitude, (c) time history of vibration velocity at $2\,\mathrm{m}$ from the track and (d) corresponding time-frequency velocity amplitude.

wheel/rail contact and the soil surface velocity at $2\,\mathrm{m}$ from the track. Using the continuous wavelet transform allows for the estimation of the localised dominant frequency [8], especially when the wheel contact interacts with the localized defect: at each wheel/defect contact, the excitation amplitude covers a large frequency range (Fig. 3(b)). However, Figure 3(d) shows that the soil vibration amplitude is greatest around $20 - 25\,\mathrm{Hz}$. This confirms recent research works [7] that the tram bogie's pitch and bounce modes significantly contribute to the generated ground vibrations. The present analysis confirms these observations and demonstrates that the bogie bounce mode is responsible for the high vibration level, as presented in Table 1.

Table 1: Main mode shapes of T2000 tram ($f_{0,i}$ and $\xi_i$ are the natural frequency and the damping ratio of mode $i$ respectively, and take the track flexibility into account).

| | leading car | central car |
|---|---|---|
| 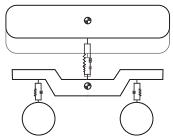 car bounce mode | $f_{0,1} = 1.8\,\mathrm{Hz}$ ($\xi_1 = 32\%$) | $f_{0,1} = 3.1\,\mathrm{Hz}$ ($\xi_1 = 55\%$) |
| 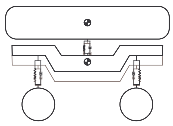 bogie bounce mode | $f_{0,2} = 19.6\,\mathrm{Hz}$ ($\xi_2 = 14\%$) | $f_{0,2} = 22.3\,\mathrm{Hz}$ ($\xi_2 = 11\%$) |
| 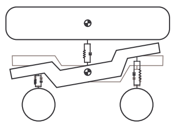 bogie pitch mode | $f_{0,3} = 29.1\,\mathrm{Hz}$ ($\xi_3 = 8\%$) | $f_{0,3} = 34.3\,\mathrm{Hz}$ ($\xi_3 = 3\%$) |
| 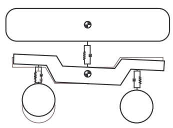 axle hop mode | $f_{0,4} = 45.5\,\mathrm{Hz}$ ($\xi_4 = 9\%$) | $f_{0,4} = 46.4\,\mathrm{Hz}$ ($\xi_4 = 9\%$) |

In order to minimise such large amplitudes, modifications can be made to the vehicle. One solution used a less-stiff material in the resilient wheels [7]; a vibration reduction of 70% was observed by dividing the original resilient material stiffness by a factor of 10! However, one drawback of this modification is the increased maintenance frequency to replace the rubber layer. Recently, Zhu et al. [9, 10] showed that the use of DVAs offers a significant reduction of vibration level, especially at frequencies close to the resonance values of floating slab tracks. The idea of the present research is to evaluate the possibility of using a DVA either in the vehicle (located close to the unsprung masses) or at the track (in the vicinity of the localized defects). The vehicle natural frequency identified from this analysis can help to tune the DVA parameters to their optimal values.

## 3. Dynamic vibration absorber design

The design procedure of a linear passive DVA for a continuous system can be based on the modal decomposition associated to the simple procedure for a single-degree-of-freedom system. The DVA is identified by its mass $m_a$, spring $k_a$ and dashpot $c_a$, associated to motion in the same direction as the undesired motion of the primary system (Fig. 4).

The primary structure — i.e. the vehicle/track subsystem — is defined by its mass $\mathbf{M}$ and stiffness $\mathbf{K}$ matrices. Among all the structure coordinates defined by the vector $\underline{\mathbf{x}}$, the coordinates $x_c$ and $x_f$ are explicitly designated, for the displacement of the points where the DVA is attached and where the

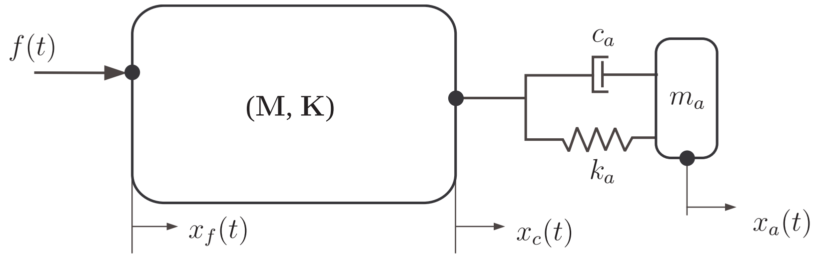


Figure 4: Schematic representation of a damped dynamic vibration absorber attached to a multi-degree-of-freedom primary system.

excitation force $f(t)$ is applied, respectively. The coordinate $x_a$ corresponds to the DVA's degree of freedom. Concerning the primary system, these coordinates can be written

$$
\begin{aligned}
x_f(t) &= \psi_{fn}\, c_n(t) && (1)\\
x_c(t) &= \psi_{cn}\, c_n(t) && (2)
\end{aligned}
$$

where $\psi_{cn}$ and $\psi_{fn}$ designate the $c^{th}$ and $f^{th}$ components of the eigenvector $\underline{\boldsymbol{\psi}}_n$ related to the mode $n$ studied, and $c_n(t)$ the associated generalized coordinate.

The orthogonality property is of course satisfied, so as

$$
\begin{aligned}
\{\underline{\boldsymbol{\psi}}_n\}^{\mathrm{T}}\ [\mathbf{M}]\ \{\underline{\boldsymbol{\psi}}_n\} &= m_n && (3)\\
\{\underline{\boldsymbol{\psi}}_n\}^{\mathrm{T}}\ [\mathbf{K}]\ \{\underline{\boldsymbol{\psi}}_n\} &= m_n\omega_n^2 && (4)
\end{aligned}
$$

where the generalized mass $m_n$ and the natural circular frequency $\omega_n$ appear.

Using the motion equations of the primary system coupled to the DVA, the decoupled equations for mode $n$ are obtained:

$$
\begin{aligned}
m_m\ddot{c}_n + c_a\psi_{cn}^2\dot{c}_n \\
-c_a\psi_{cn}\dot{x}_a + (m_m\omega_n + k_a\psi_{cn}^2)c_n - k_a\psi_{cn}x_a &= \psi_{fn}f(t) && (5)\\
m_a\ddot{x}_a + c_a\dot{x}_a - c_a\psi_{cn}\dot{c}_n + k_a x_a - k_a\psi_{cn}c_n &= 0\,. && (6)
\end{aligned}
$$

This approach allows the differential equations to be decoupled using the modal base.

At this stage, it is preferable to use the concept of effective mass $m_{n,\mathrm{eff}}$ and effective stiffness $k_{n,\mathrm{eff}}$

$$
\begin{aligned}
m_{n,\mathrm{eff}} &= \frac{m_n}{\psi_{cn}^2} && (7)\\
k_{n,\mathrm{eff}} &= \frac{m_n\omega_n^2}{\psi_{cn}^2} && (8)
\end{aligned}
$$

to be invariant to the normalization procedure adopted for the eigenvector $\underline{\boldsymbol{\psi}}_n$.

The primary response is thus summarized by the following frequency response function (FRF), obtained from Eqs. (5), (6) and (2), after Fourier transformation:

$$
\frac{|X_c|}{F_0} = \frac{\psi_{cn}\psi_{fn}}{k_{n,\mathrm{eff}}}\sqrt{\frac{(2\xi_n\Omega)^2 + (\Omega^2-\varphi^2)^2}{(2\xi_n\Omega)^2(1-\Omega^2-\mu_n\Omega^2)^2 + \left[\mu_n\varphi^2\Omega^2 - (\Omega^2-1)(\Omega^2-\varphi^2)\right]^2}} \qquad (9)
$$

where $X_c$ and $F_0$ represent the Fourier transform of $x_c(t)$ and $f(t)$, respectively, and where the following adimensional parameters are introduced:

$$\Omega = \frac{\omega}{\omega_n} \qquad \text{(forcing frequency ratio)} \tag{10}$$

$$\varphi = \frac{\omega_a}{\omega_n} \qquad \text{(tuning factor)} \tag{11}$$

$$\mu_n = \frac{m_a}{m_{n,\mathrm{eff}}} \qquad \text{(mass ratio)} \tag{12}$$

$$\xi_n = \frac{c_a}{2m_a\omega_n} \qquad \text{(damping ratio)} \tag{13}$$

with the natural circular frequency of the DVA:

$$\omega_a = \sqrt{\frac{k_a}{m_a}}\,. \tag{14}$$

This procedure allows the study to be focused around the mode $n$, corresponding to the tram bounce mode. Particularly, Den Hartog's optimisation formulas [11] identify the best value of the tuning factor and damping ratio as a function of the mass ratio:

$$\varphi_{\mathrm{opt}} = \frac{1}{1+\mu}\,, \tag{15}$$

$$\xi_{\mathrm{opt}} = \sqrt{\frac{3\mu}{8(1+\mu)^3}}\,. \tag{16}$$

Note that Eq. (16) is only valid for an undamped primary system. Tabulated optimal damping ratios can be found in literature (e.g. [12]). However, the damping structure can be introduced in the present analysis using the Rayleigh damping definition defined as a combination of the mass $\mathbf{M}$ and stiffness $\mathbf{K}$ matrices:

$$[\mathbf{C}] = \alpha\,[\mathbf{M}] + \beta\,[\mathbf{K}] \tag{17}$$

In this formulation, the coefficients $\alpha$ and $\beta$ are selected to match the damping ratio at two specific frequencies including the natural frequency $f_n$ [13]. This extended approach has been applied in the present application, without observing a significant difference in the DVA parameters.

## 4. Results

### 4.1 Dynamic vibration absorber on vehicle

The initial analysis was focused on the DVA placed on the vehicle. The mass value $m_a$ was fixed to $100\,\mathrm{kg}$, sufficiently realistic for the present case. Various simulations showed that the best location of the DVA is on the bogie and the main mode to attenuate is the bogie bounce mode, with the following DVA values: $k_a = 1.3\,\mathrm{MN/m}$ and $c_a = 4.1\,\mathrm{kNs/m}$ (leading car with the tuned DVA frequency $f_a = 18.2\,\mathrm{Hz}$) and $k_a = 1.8\,\mathrm{MN/m}$ and $c_a = 4.7\,\mathrm{kNs/m}$ (middle car with $f_a = 21.2\,\mathrm{Hz}$). Two different DVA parameters were obtained as the corresponding eigenfrequency is different for each car. Figure 5 shows the calculated FRF at the motorised wheel with and without the DVA, obtained from the aforementioned vehicle/track model. A clear amplitude reduction of $2\,\mathrm{dB}$ is observed for these bounce mode peaks without modifying the other structure's mode. For the leading bogie, the modified mode is transformed into two modes at $16.4$ and $21.7\,\mathrm{Hz}$, with increased levels of damping ($19.2$ and $24.6\,\mathrm{Hz}$ for the middle car).

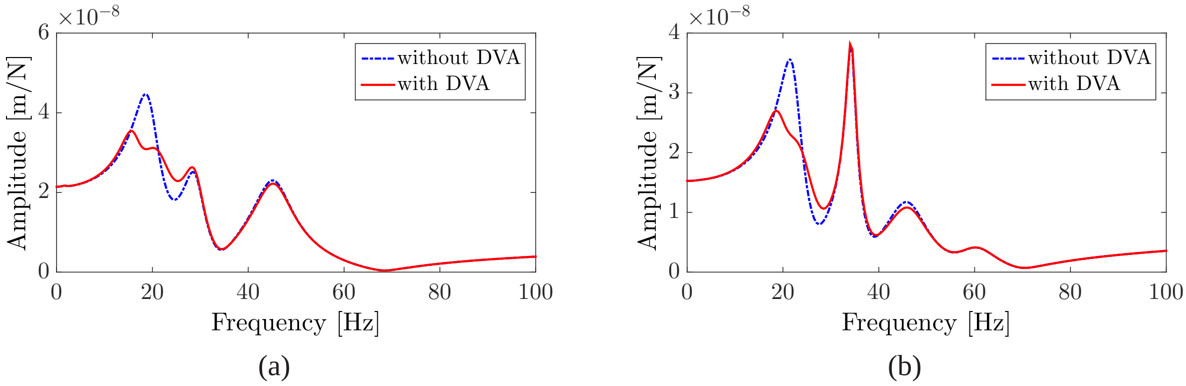


Figure 5: The frequency response functions at the motorised wheel (driving point) with and without dynamic vibration absorbers at the vehicle bogie: (a) leading car and (b) middle car.

### 4.2 Dynamic vibration absorber on track

The second analysis focused on the placement of the DVAs on the track (Fig. 6). Two possible locations were examined: on the rail or on a sleeper, both within the vicinity of the localized defect. One gain, the bogie bounce mode is the most critical issue and a DVA mass of $m_a = 100\,\mathrm{kg}$ was also selected. Because of the different car modal characteristics, two DVAs are necessary (one tuned to the corresponding mode of the leading cars and one tuned to the mode of the middle car). Compared to the previous simulation, the gain is less visible. This is mainly due to the low DVA mass values with mass ratios of $\mu = 0.01$ and $\mu = 0.001$ for the rail and the sleeper, respectively (divided by 10 and 100, compared to the mass ratio of the DVA on the vehicle). Additional simulations could confirm these observations, including the prediction of the ground vibrations with the modified track structure.

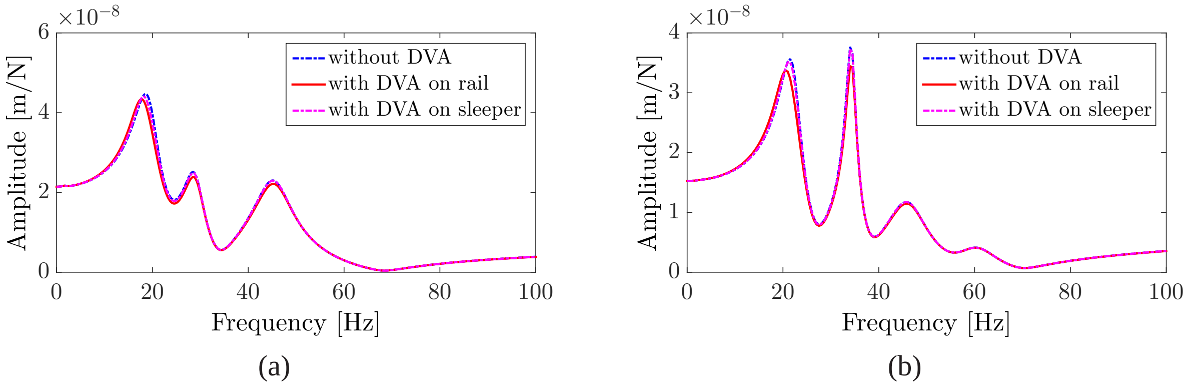


Figure 6: The frequency response functions at the motorised wheel (driving point) with and without dynamic vibration absorbers placed on the track in the vicinity of the localized defect: (a) leading car and (b) middle car.

## 5. Conclusions

A design of DVAs was carried out in order to evaluate the potential of such mitigation measures in the case of urban conditions. The ground vibrations induced by a localized defect was retained in order to calibrate such a device. From this study, the following observations can be drawn:

- A direct correlation between the excitation forces and the ground vibration velocities in the time-frequency scale allowed the main vehicle mode to be identified as the principal contributor

to excessive levels of vibration.
- The modal decomposition applied to the vehicle/track model offers a way to obtain the optimal DVA parameter values for any location.
- From the FRFs, it turns out that a DVA placed on the vehicle, close to the excitation contributor, is more efficient than DVAs located on the track, even close to the localized defect.

Further investigations, including a complete analysis of the vehicle/track/soil model, could confirm the last finding and provide a significant gain in terms of ground vibration level reduction.

## Acknowledgement

This work was supported by the Chinese National Program of Introducing Talents of Discipline to Universities — 111 Project (Grant No. B16041).

## REFERENCES

1. Vogiatzis, K. and Kouroussis, G., (2017), Airborne and ground borne noise and vibration from urban rail transit systems. *Urban transport systems*, pp. 61–87, InTech.
2. Kouroussis, G., Connolly, D. P., Alexandrou, G. and Vogiatzis, K. The effect of railway local irregularities on ground vibration, *Transportation Research — Part D: Transport and Environment*, **39**, 17–30, (2015).
3. Vogiatzis, K. E. and Kouroussis, G. Environmental ground borne noise and vibration from urban light rail transportation during construction and operation, *Current Pollution Reports*, **3** (2), 162–173, (2017).
4. Kouroussis, G., Van Parys, L., Conti, C. and Verlinden, O. Prediction of ground vibrations induced by urban railway traffic: an analysis of the coupling assumptions between vehicle, track, soil, and buildings, *International Journal of Acoustics and Vibration*, **18** (4), 163–172, (2013).
5. Kouroussis, G., Vogiatzis, K. E. and Connolly, D. P. A combined numerical/experimental prediction method for urban railway vibration, *Soil Dynamics and Earthquake Engineering*, **97**, 377–386, (2017).
6. Kouroussis, G., Vogiatzis, K. and Connolly, D. P. Assessment of railway ground vibration in urban area using in-situ transfer mobilities and simulated vehicle-track interaction, *International Journal of Rail Transportation*, **6** (2), 113–130, (2018).
7. Kouroussis, G., Verlinden, O. and Conti, C. Efficiency of resilient wheels on the alleviation of railway ground vibrations, *Journal of Rail and Rapid Transit*, **226** (4), 381–396, (2012).
8. Ainalis, D., Ducarne, L., Kaufmann, O., Tshibangu, J.-P., Verlinden, O. and Kouroussis, G. Improved analysis of ground vibrations produced by man-made sources, *Science of the Total Environment*, **616-617**, 517–530, (2018).
9. Zhu, S., Yang, J., Cai, C., Pan, Z. and Zhai, W. Application of dynamic vibration absorbers in designing a vibration isolation track at low-frequency domain, *Proceedings of the Institution of Mechanical Engineers, Part F: Journal of Rail and Rapid Transit*, **231** (5), 546–557, (2017).
10. Zhu, S., Wang, J., Cai, C., Wang, K., Zhai, W., Yang, J. and Yan, H. Development of a vibration attenuation track at low frequencies for urban rail transit, *Computer-Aided Civil and Infrastructure Engineering*, **32** (9), 713–726, (2017).
11. Den Hartog, J. P., *Mechanical vibrations*, McGraw-Hill, New York (USA), 4$^{\text{th}}$ edn. (1956).
12. Steffen Jr., V. and Rade, D., (2001), Vibration absorbers. Braun, S. (Ed.), *Encyclopedia of Vibration*, pp. 9–26, Elsevier.
13. Kouroussis, G., Ben Fekih, L., Bottieau, J.-Y. and Verlinden, O. Structural response of a vertical-axis wind turbine equipped with a vibration neutraliser, *20th International Congress on Sound and Vibration (ICSV20)*, Bangkok (Thailand), (2013).